



# Tailoring the Structural and Optical Features of PVA/SiO<sub>2</sub>-CuO Polymeric Nanocomposite for Optical and Gamma Ray Shielding Applications

Idrees Oreibi<sup>1</sup> · Majeed Ali Habeeb<sup>2</sup> · Rehab Shather Abdul Hamza<sup>2</sup>

Received: 21 July 2023 / Accepted: 14 November 2023 / Published online: 21 November 2023  
© The Author(s), under exclusive licence to Springer Nature B.V. 2023

## Abstract

This study aims to produce novel nanocomposite films by incorporating nanostructures (SiO<sub>2</sub> and CuO) into polyvinyl alcohol (PVA) to utilize these nanocomposites in various optoelectronic nanodevices. The PVA/SiO<sub>2</sub>-CuO nanostructures exhibit notable attributes such as low cost, enhanced corrosion resistance, favorable optical properties, and reduced weight compared to alternative nanosystems. This study focused on investigating the structural and optical properties of nanostructures composed of PVA/SiO<sub>2</sub>-CuO. The FTIR spectra suggest the presence of a physical interaction between the pristine polymer and nanoparticles. The optical microscope was utilized to analyze the nanocomposite's structural characteristics and surface morphology alterations. The findings about the optical characteristics indicate a notable increase of approximately 180% in absorption, accompanied by a decrease of about 48% in the energy gap for allowed indirect transitions and 72% for forbidden indirect transitions. These changes were observed when the PVA/SiO<sub>2</sub>-CuO content reached a weight percentage of 6%. Consequently, this material exhibits potential suitability for various optoelectronic devices, such as photovoltaic cells, solar cells, diodes, transistors, lasers, electronic gates, and other fields. The optical characteristics of polyvinyl alcohol (PVA) were enhanced as the concentration of SiO<sub>2</sub>-CuO nanoparticles (NPs) increased, leading to improvements in the absorption coefficient ( $\alpha$ ), refractive index ( $n$ ), extinction coefficient ( $k$ ), real ( $\epsilon_1$ ) and imaginary ( $\epsilon_2$ ) parts of the dielectric constants, optical conductivity ( $\sigma_{op}$ ), and dispersion factors. The prepared nanocomposites underwent testing to evaluate their effectiveness in shielding gamma rays. The experimental findings indicate that the nanocomposite films of PVA/SiO<sub>2</sub>-CuO exhibit significant attenuation coefficients when exposed to gamma rays. Thus, it can be seen that incorporating (SiO<sub>2</sub>-CuO) NPs has enhanced the optical properties of the resulting nanocomposite, and this material can be considered a promising material for flexible optoelectronic applications and gamma ray shielding.

**Keywords** Nanocomposites · Optical properties · SiO<sub>2</sub>-CuO nanoparticles · Gamma ray attenuation

## 1 Introduction

Nanotechnology is a rapidly developing discipline in the twenty-first century, wherein nanoparticles possess unique structural, optical, electrical, magnetic, and mechanical properties attributable to their nanoscale dimensions ranging from 1 to 100 nm, in contrast to their larger bulk counterparts [1]. There has been a notable surge in interest surrounding metal oxide nanoparticles, primarily due to their extensive utilization as catalysts in industrial settings, antimicrobial agents, medical applications, fillers, chemical sensors, disinfectants, semiconductors, catalysts, and their significant contributions to the advancement of cosmetics and microelectronics [2, 3]. Metal oxide nanoparticles, including copper oxide (CuO), have garnered significant interest due

✉ Majeed Ali Habeeb  
pure.majeed.ali@uobabylon.edu.iq

Idrees Oreibi  
idrees114af@gmail.com

Rehab Shather Abdul Hamza  
alamerirehab300@gmail.com

<sup>1</sup> Ministry of Education, Hilla, Babil, Iraq

<sup>2</sup> College of Education for Pure Sciences, Department of Physics, University of Babylon, Hilla, Babil, Iraq

to their antimicrobial and biocidal characteristics, rendering them potentially valuable in various biomedical contexts [4]. Copper oxide is categorized as a semiconductor metal owing to its unique optical, electrical, and magnetic properties. The substance above has been utilized in various fields, including advancing supercapacitors, near-infrared filters, catalytic processes, sensors, magnetic storage mediums, and semiconductors, among other applications [5, 6]. Copper oxide nanoparticles (CuO NPs) have been employed to enhance polymer films, whether derived from petro-based or bio-based polymers; this is due to the notable attributes of CuO NPs, including their elevated surface-to-volume ratio, relatively reduced toxicity, ability to reinforce the mechanical properties of polymers and thermal stability [7]. Integrating polymers into various aspects of human existence has become indispensable, as it is arduous to envision a viable existence devoid of the manifold services facilitated by these versatile materials [8, 9]. Polymers are widely used in diverse electronic strategies and applications because of their distinct properties, including facile reconfigurability, flexibility, high resistance, and cost-effectiveness, alongside other significant properties [10]. Silicon dioxide ( $\text{SiO}_2$ ), or silica, is a versatile material utilized in various industries, naturally occurring and synthetically produced. Its widespread application in numerous sectors necessitates further exploration [11]. Silicon oxide NPs have unique physical, chemical, and optical properties that can be applied in many fields. Silicon dioxide exhibits notable attributes such as high hardness and thermal stability, which can potentially compensate for the deficiencies associated with low bearing capacity and inadequate wear resistance of lubricants [12].

Furthermore, silicon dioxide ( $\text{SiO}_2$ ) is a substance lacking a crystalline structure and possesses properties that render it harmless to living organisms. It exhibits a wide range of potential uses in numerous fields. Silica, in its various manifestations, is a solid substance characterized by its lack of scent and composed of silicon and oxygen atoms. Silica particles become airborne and aggregate to form non-combustible particulate matter [13, 14]. Integrating  $\text{SiO}_2$  particles into the composite polymer leads to higher chemical and mechanical properties and improved dimensional stability. These particles serve as solid plasticizers [15].

Polyvinyl alcohol (PVA) has emerged as a promising host matrix for a wide range of metal oxide nanofillers due to its biodegradability, non-toxicity, ability to form films, ease of processing, optical transparency, minimal light scattering with a low refractive index, and impressive mechanical properties [16, 17]. PVA is a water-soluble synthetic polymer that comes as a granular powder that is odorless, translucent, tasteless, and white or cream in color. Since PVA is water-soluble, it can be used to make hydroxyl organic ingredients. PVA's biological degradation and biocompatibility are two of its most notable characteristics. PVA has a high tensile

strength and longevity and a high oxygen and scent buffer. Visual light transmission is excellent. It also has excellent shape, mixing, and adhesion characteristics [18]. Polyvinyl alcohol (PVA) is often subjected to annealing methods using a wide range of low-molecular-weight chemicals that often contain polarised groups. These groups form hydrogen bonds with the hydroxyl groups of the PVA chain, regardless of the presence or absence of water, resulting in a reduction in direct hydrogen bonding between the bigger PVA molecules [19, 20]. The investigation of gamma-radiation shielding is a promising area of study due to the hazardous impact of gamma rays on human well-being. Various materials, including concrete and glass, were employed to shield against  $\gamma$ -rays. In order to attain desirable properties of  $\gamma$ -radiation and X-ray attenuation in nanocomposites, a combination of recycled thermoplastics and inorganic nanofillers was employed [21, 22].

D.E. Abulyazied et al., in (2022) [23], have studied the effect of molybdenum nanoparticles (Mo-NPs) on the radiation protection properties of polyvinyl alcohol (PVA) for gamma shielding application. Zainab et al., in (2023) [24], the present study focuses on the investigation of novel nanocomposites, including polyvinyl alcohol (PVA) and varying concentrations (0, 1, 2, and 3 wt%) of cobalt oxide and zirconium dioxide ( $\text{CoO-ZrO}_2$ ) nanoparticles. The casting process was employed as the chosen technique for synthesizing and fabricating these nanocomposites. A. A. Alhazime, in (2020) [25], studied the effect of nano CuO doping on the structural, thermal and optical properties of PVA/PEG blend prepared by casting technique.

The novelty of this study lies in the novel combination of  $\text{SiO}_2$  and CuO nanoparticles with PVA, resulting in a unique nanocomposite. The material's versatility is evident in potential applications such as photovoltaic cells and gamma radiation shielding. Additionally, the concentration-dependent analysis provides valuable insights into tailoring properties for specific uses, making it a noteworthy contribution to nanocomposite research. To our knowledge, no attempt has been made to synthesize nanocomposites including  $\text{SiO}_2$ -CuO nanoparticles.

This paper aims to present the low-cost and easy synthesis process by (PVA/ $\text{SiO}_2$ -CuO) nanostructures for optoelectronics and gamma ray shielding applications.

## 2 Materials and Methods

Nanocomposite films were produced by employing the casting method, utilizing polyvinyl alcohol (PVA), silicon dioxide ( $\text{SiO}_2$ ), and copper oxide (CuO) nanoparticles. Polyvinyl alcohol (PVA) was used in powder form and obtained from Panveac Spain company with high purity (99.8%). Silicon dioxide ( $\text{SiO}_2$ ) is widely utilized in biomedical research owing to its

favorable attributes, including low toxicity, stability, and amenability to functionalization with diverse chemicals and polymers. The silicon dioxide nanopowder was obtained from US Research Nanomaterials, Inc, with a grain size of 60 nm and high purity of 99.9%. It appears in the form of white powder. The copper oxide nanopowder, denoted as CuO, was acquired in powder form from Zhengzhou Dongyao Nano Materials in China. The powder has a grain size of 50 nm and exhibits a high purity level, precisely 99.9%. The process involved dissolving pure PVA in 40 ml of distilled water for 50 min while stirring with a magnetic stirrer at 65 °C to achieve a more homogeneous solution. The polymer blend was subjected to the addition of nanoparticles of silicon dioxide (SiO<sub>2</sub>) and copper oxide (CuO) at varying concentrations of [0%, 2% wt. (0.5%SiO<sub>2</sub>/1.5%CuO), 4% wt. (1%SiO<sub>2</sub>/3%CuO), and 6% wt. (1.5%SiO<sub>2</sub>/4.5%CuO)]. Following a three-day drying period at a temperature of 25 °C, the result was the successful synthesis of polymer nanocomposites. The nanocomposites consisting of PVA/SiO<sub>2</sub>-CuO were retrieved from the petri dish and employed for subsequent measurement. Fourier transform infrared spectroscopy (FTIR) is employed to assess nanocomposites of (PVA/SiO<sub>2</sub>-CuO) samples. The evaluation is conducted within 1000 to 4000 cm<sup>-1</sup> wave number range. The samples underwent testing at different concentrations using an Olympus-type Nikon-73346 optical microscope, which had a magnification of 10× and was equipped with a camera for microscopic photography. The optical characteristics of PVA, SiO<sub>2</sub>, and CuO nanocomposites were analyzed within the 200–800 nm wavelength range using a UV/1800/Shimadzu spectrophotometer. The specimens were placed in the path of a collimated beam emitted by gamma ray sources, specifically Cs-137, with an activity of 5mCi. The distance between the gamma ray source and the detector is 2 cm. The linear attenuation coefficients were determined by utilizing Geiger counter measurements to evaluate the transmitted gamma ray fluxes through nanocomposites consisting of (PVA/SiO<sub>2</sub>-CuO) NCs.

Absorbance is calculated by using relation [26]

$$A = I_A/I_o \quad (1)$$

Where:  $I_A$  is the absorbed light intensity, and  $I_o$  is the incident intensity of light.

Transmittance is calculated by using relation [27]

$$T_r = I_{Tr}/I_o \quad (2)$$

Where:  $I_{Tr}$  is the intensity of Transmitted light, and  $I_o$  is the incident intensity of light.

Absorption coefficient ( $\alpha$ ) calculated from equation [27]

$$\alpha = (2.303 \times A)/d \quad (3)$$

Where  $d$  is the sample thickness (0.14 mm), and  $A$  is the absorption of the material.

The indirect transition is calculated by using relation [28]

$$\alpha h\nu = B(h\nu - E_g)^r \quad (4)$$

Where  $B$  is constant,  $h\nu$  is the incident photon energy,  $E_g$  is the optical band gap, and  $r$  is 2 for allowed indirect transitions and 3 for forbidden indirect transitions.

The extinction coefficient ( $k$ ) was calculated using the following equation [29]

$$k = \frac{\alpha\lambda}{4\pi} \quad (5)$$

Where:  $\lambda$  is the wavelength.

The refractive index ( $n$ ) is calculated from equation [30]

$$n = \sqrt{4R - \frac{k^2}{(R-1)^2} - \frac{(R+1)}{(R-1)}} \quad (6)$$

Where:  $R$  is the reflectance.

The dielectric constant (real and imaginary parts) is calculated by [31]

$$\epsilon_1 = n^2 - k^2 \quad (7)$$

$$\epsilon_2 = 2nk \quad (8)$$

The optical conductivity ( $\sigma_{op}$ ) is obtained by using the relation [32]

$$\sigma_{op} = \alpha nc/4\pi \quad (9)$$

Where:  $c$  is the velocity of light.

The equation presented below can be utilized to derive the linear attenuation coefficients ( $\mu$ ) based on the material thicknesses [33]

$$N = N_o e^{-\mu d} \quad (10)$$

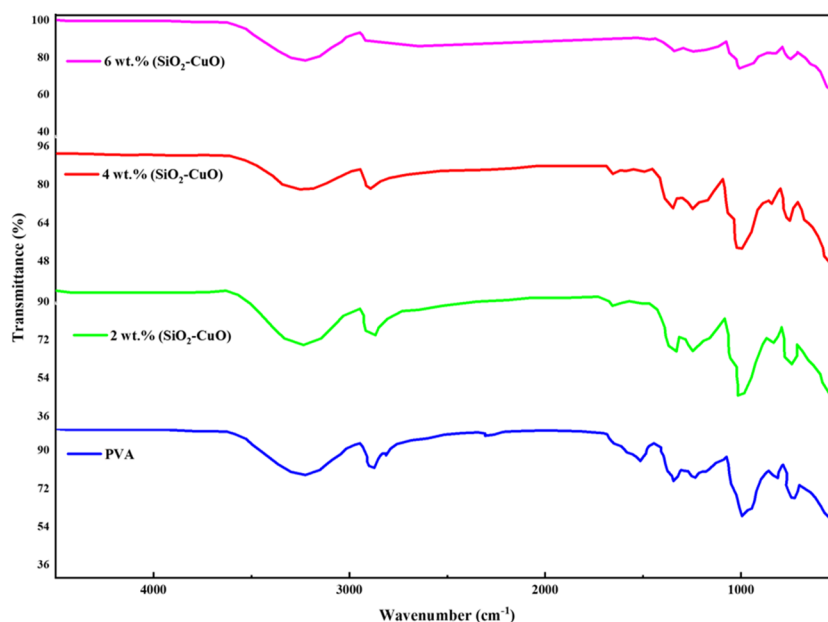
where  $N_o$  is a gamma ray incident,  $N$  is the attenuation of the gamma rays, and  $d$  is the thickness of the sample.

## 3 Results and Discussion

### 3.1 Fourier Transform Infrared Ray (FTIR) Analysis of (PVA/SiO<sub>2</sub>-CuO) NCs

The transmittance spectra of nanocomposite films containing (PVA/SiO<sub>2</sub>-CuO) were recorded at room temperature using Fourier transform infrared spectroscopy (FTIR). Figure 1 illustrates these spectra, which cover a range of 600 to 4500 cm<sup>-1</sup>. Figure 1 displays the three distinct regions within the infrared (IR) spectra that are associated with pure polyvinyl alcohol (PVA). The initial specimen exhibits a broad absorption spectrum, with a peak at 3250 cm<sup>-1</sup>. This peak is attributed to the stretching of the hydroxyl group (O-H), characterized by a robust bond strength. The occurrence of

**Fig. 1** FTIR spectra for (PVA/SiO<sub>2</sub>-CuO) nanocomposites



this peak at a higher range of wavelengths further emphasizes its significance. The second spectral region manifests at a wavenumber of  $2900\text{ cm}^{-1}$ , indicating the presence of bonding interactions of moderate strength. The observed peaks in this region indicate the existence of C-H stretching within the PVA structure. The third region corresponds to weak intermolecular bonds and is observed within the lower wavelength range of approximately  $1000\text{--}1500\text{ cm}^{-1}$ , indicative of C-O stretching. The additional peaks observed in the depicted graph, located at approximately  $1650$ ,  $900$ ,  $800$ , and  $500\text{ cm}^{-1}$ , can be attributed to the bending of C=C stretching, CH<sub>3</sub> groups, CC stretching vibrations, and Wagging mode of (OH) groups.

Similarly, the peaks observed at around  $1400\text{ cm}^{-1}$  indicate the deformation of O-CH<sub>3</sub> groups. Furthermore, the peak observed at  $1080\text{ cm}^{-1}$  corresponds to the stretching vibrations of O-CH<sub>2</sub> groups, which are also inherent to the structure of PVA, as shown in Table 1. In this study, Fig. 1 illustrate the application of Fourier Transform Spectroscopy (FTIR) to analyze the characteristics of pure Polyvinyl Alcohol (PVA) samples doped with varying proportions of silicon dioxide (SiO<sub>2</sub>) and copper oxide (CuO) nanoparticles. The analysis was conducted for both groups. The treatment applied to the samples led to noticeable alterations in their spectral characteristics. Specifically, new absorption bands emerged, and the intensity of pre-existing absorption bands increased; this indicates decoupling between the corresponding vibrations due to interaction between (SiO<sub>2</sub>-CuO) nanoparticles and the polymers. The increased density of the films with more nanoparticles added means more atoms and ions in the light path and thus increased absorbance. The emergence of novel bands can be

**Table 1** FTIR Transmittance bands positions and their assignments

Wavenumber (cm <sup>-1</sup> )	Band assignment
3250	hydroxyl group (O-H) [36]
2900	C-H stretching [36]
1650	C=C stretching [37]
1500	C-O stretching [32]
1400	O-CH <sub>3</sub> groups [35]
1080	O-CH <sub>2</sub> groups [35]
900	CH <sub>3</sub> groups [32]
800	CC stretching vibrations [37]
500	Wagging mode of (OH) groups [37]

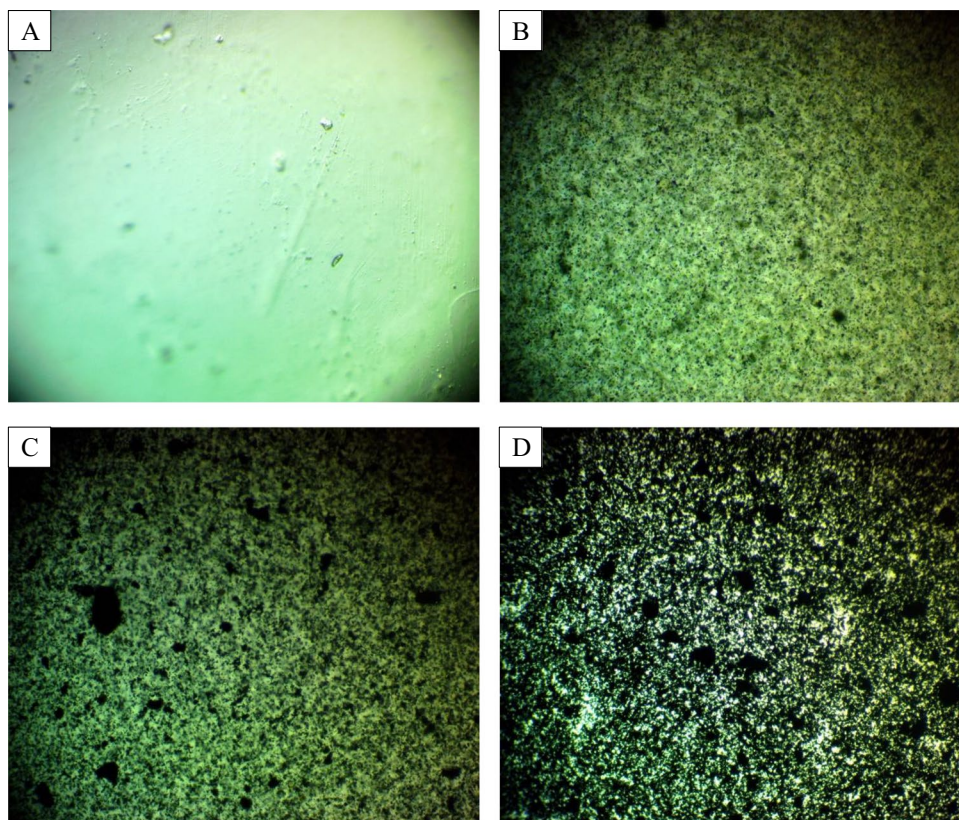
attributed to defects resulting from the charge transfer interaction between the pristine polyvinyl alcohol (PVA) chains and the nano dopant, which changes the PVA's molecular structure [34, 35].

### 3.2 Optical Microscope of (PVA/SiO<sub>2</sub>-CuO) Nanocomposites

Figure 2 displays the photomicrographs of the surface of pure polyvinyl alcohol (PVA) and its nanocomposites (NCs) containing varying weight percentages (wt.%) of silicon dioxide-copper oxide (SiO<sub>2</sub>-CuO) nanoparticles (NPs) at a magnification power of 10x. The observed surface image of the polymer blend film depicted in part (A) suggests a uniform phase without any discernible phase separation. In other words, the film exhibits a finer morphology with a smooth surface, indicating the remarkable miscibility of polyvinyl alcohol (PVA) at this specific blend ratio. Based



**Fig. 2** Photomicrographs (10x) for (PVA/SiO<sub>2</sub>-CuO) NCs: **(A)** for pure PVA, **(B)** for 2 wt% (SiO<sub>2</sub>-CuO), **(C)** for 4 wt% (SiO<sub>2</sub>-CuO), **(D)** for 6 wt% (SiO<sub>2</sub>-CuO)



on the observations made from the provided figure (part B-D), it is evident that the (SiO<sub>2</sub>-CuO) nanoparticles exhibit a uniform distribution across the polymer film surface. This characteristic becomes more pronounced as the weight percentage (wt.%) of (SiO<sub>2</sub>-CuO) increases. The NCs exhibit an almost elliptical arrangement of particles with a consistent shape. This phenomenon can be attributed to the significant surface area of the nanoparticles (NPs) and various polar groups in the polymeric solution [38]. The polymeric solution exhibits a strong affinity for the (SiO<sub>2</sub>-CuO) material, resulting in the alignment of the nanoparticles along the polymer chain. Consequently, the nanocomposite structure becomes denser, enhancing material consistency. This methodology offers an appropriate approach for preparing non-conventional films [39].

### 3.3 The Optical Properties of (PVA/SiO<sub>2</sub>-CuO) Nanocomposites

Incorporating nanoparticles into the polymer matrix regulates the optical band gap, diminishing its magnitude and enabling its utilization in diverse applications. Furthermore, adding SiO<sub>2</sub>-CuO NPs to polymers significantly enhances their optical properties. For example, SiO<sub>2</sub>-CuO NPs can affect light refraction and scattering as it passes through the polymer, leading to changes in optical properties such as refraction. When light interacts with NPs, phenomena

called Surface Enhanced Effects can occur, which amplify the light's effects and allow for overall optical enhancement. Under the influence of these NPs, changes in color, contrast, and refraction of light can occur. Furthermore, NPs can be used to design precise nano-level structural arrangements, which control the interaction of light with the polymer and enhance its optical effects in various ways, such as improving light emission or increasing light absorption. In general, the optical properties of polymers are improved by incorporating appropriate NPs and designing nanometer-scale structures that effectively influence the interaction of light with the polymer.

Figure 3 depicts the UV-Vis-NIR absorption spectra of polyvinyl alcohol (PVA) and its nanocomposites (NCs) containing varying weight percentages (wt.%) of (SiO<sub>2</sub>-CuO) nanoparticle films. NPs can be used to design precise nano-level structural arrangements, which control the interaction of light with the polymer and enhance its optical effects in various ways, such as improving light emission or increasing light absorption. The measurements were conducted within the wavelength range of 190–1100 nm. Adding (SiO<sub>2</sub>-CuO) nanoparticles resulted in a shift of the absorption edge towards the higher wavelength side in NCs films, reducing the energy gap. This phenomenon can be attributed to alterations in the mobility of polymeric chains during the blending procedure [40]. The prominent characteristic of (SiO<sub>2</sub>-CuO) in the polymer is its efficient ultraviolet (UV) absorption,

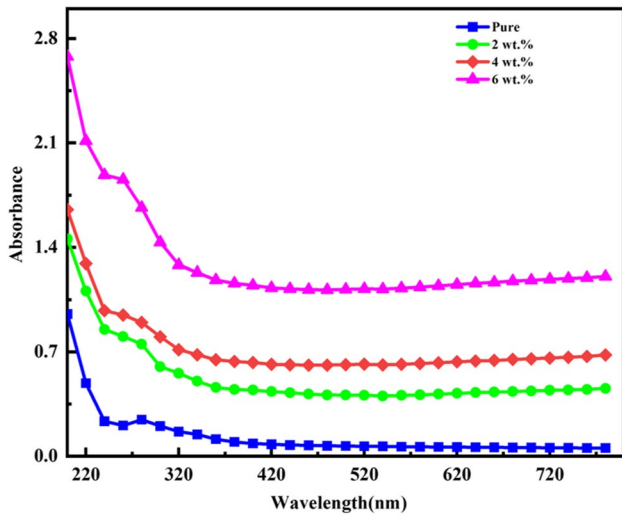


**Fig. 3** Absorbance of (PVA/SiO<sub>2</sub>-CuO) NCs as a function of wavelength

which can be attributed to its substantial energy gap. The absorption capacity of NCs surpasses that of pure polyvinyl alcohol (PVA). The enhanced absorption can be ascribed to the interfacial interaction between the nanoparticles and the adjacent polar groups of polyvinyl alcohol (PVA), which aligns with previously documented observations [41].

Figure 4 illustrates the relationship between the transmittance of (PVA/SiO<sub>2</sub>-CuO) nanocomposites and the wavelength of the incident light. As depicted in the figure, there is a noticeable correlation between the concentration of (SiO<sub>2</sub>-CuO) nanoparticles and both absorbance and transmittance. Specifically, as the concentration increases, the absorbance values rise while the transmittance values

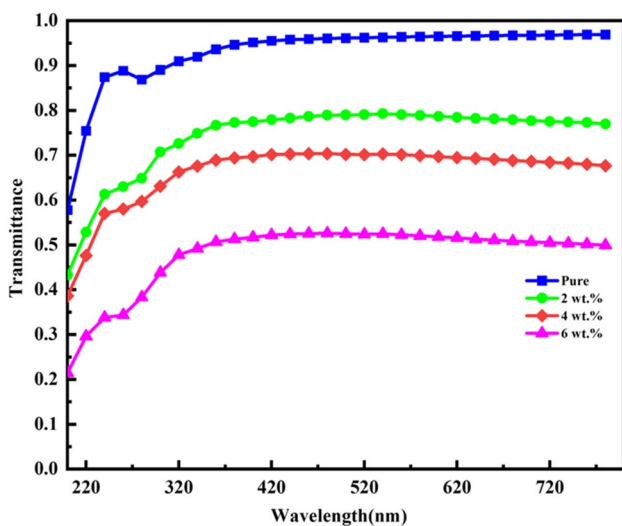


**Fig. 4** Shows the transmission spectra of (PVA/SiO<sub>2</sub>-CuO) NCs as a function of wavelength

decline. This phenomenon can be attributed to the agglomeration of nanoparticles at higher concentrations, leading to increased charge carriers due to several effects. One of these effects is the increased available surface area for interactions with charged materials, which raises the likelihood of capturing and trapping charges.

Additionally, nanoparticles can improve the distribution of charges within the polymer matrix and reduce their aggregation, thereby enhancing charge conductivity. These changes make polymers loaded with nanoparticles ideal for applications requiring efficient charge transport and distribution, such as electronic devices and solar cells [42]. The decrease in transmittance is also due to the nature of refractions and reflections within the material itself. This behavior agrees with the results of the researcher [43].

Figure 5 depicts the relationship between the absorption coefficient of (PVA/SiO<sub>2</sub>-CuO) nanocomposites and the ratios of SiO<sub>2</sub>-CuO NPs. It is observed that the absorption coefficient increases as the ratios of SiO<sub>2</sub>-CuO NPs increase. This phenomenon can be attributed to the rise in charge carriers within the nanocomposite films [44]. The absorption coefficient ( $\alpha$ ) for all the prepared nanocomposites exhibited the lowest values at low energies, which could be attributed to the limited likelihood of electron transitions. The probability of electron transition is high when the energy of the incident photon increases, indicating that the energy of the incident photon is adequate for atom interaction. Based on the observed  $\alpha$  values of the prepared films, which are less than  $10^4 \text{ cm}^{-1}$ , it can be inferred that indirect electronic transitions are highly probable [45].

Figure 6 illustrates the correlation between the square root of the absorption edge ( $\alpha h\nu$ )<sup>1/2</sup> for nanocomposites consisting of polyvinyl alcohol (PVA) and silicon dioxide-copper

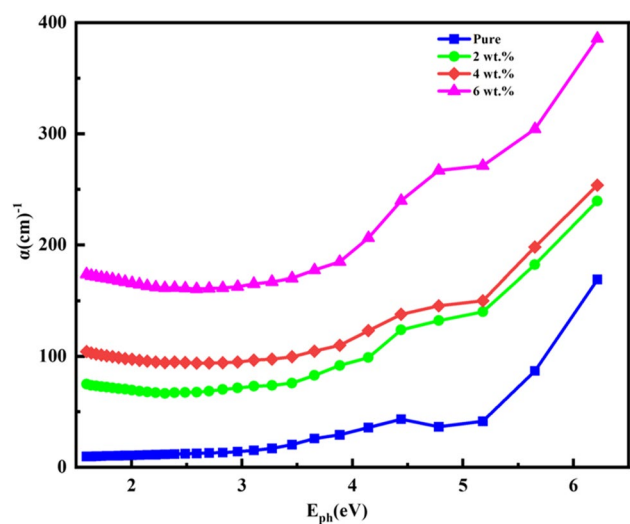


**Fig. 5** Absorption coefficient for (PVA/SiO<sub>2</sub>-CuO) NCs as a function of photon energy

oxide (SiO<sub>2</sub>-CuO) and the energy of the incident photons. By extending a straight line from the highest point of the curve to intersect the x-axis at  $(\alpha h\nu)^{1/2} = 0$ , we can determine the energy gap associated with the permissible indirect transition. The values obtained are presented in Table 2. The energy gap values exhibit a decreasing trend as the weight percentages of (SiO<sub>2</sub>-CuO) nanoparticles increase. Incorporating nanoparticles into the polymer matrix regulates the optical band gap, diminishing its magnitude and enabling its utilization in diverse applications. This phenomenon is responsible for forming localized states within the forbidden energy gap. In the present situation, the transfer process unfolds biphasically, involving the migration of an electron from the valence band to the local levels, followed by its subsequent transition to the conduction band. This progression is observed to be directly influenced by the weight percentage of (SiO<sub>2</sub>-CuO) nanoparticles. The observed behavior can be attributed to the heterogeneous composition of nanocomposites, wherein the electronic conduction is contingent upon the concentration of added components. It is noted that the density of localized states exhibits an increase as the concentration of (SiO<sub>2</sub>-CuO) nanoparticles is raised [46, 47].

Figure 7 illustrates the correlation between the cubic root of the product of the fine structure constant ( $\alpha$ ), Planck's constant ( $h$ ), and the frequency ( $\nu$ ), denoted as  $(\alpha h\nu)^{1/3}$ , and the energy of photons in nanocomposites. The image illustrates a clear correlation between the concentration of (SiO<sub>2</sub>-CuO) nanoparticles and the energy gap values for forbidden indirect transitions. Specifically, it shows a consistent decrease in energy gap values as the concentration of nanoparticles increases. Moreover, the magnitudes

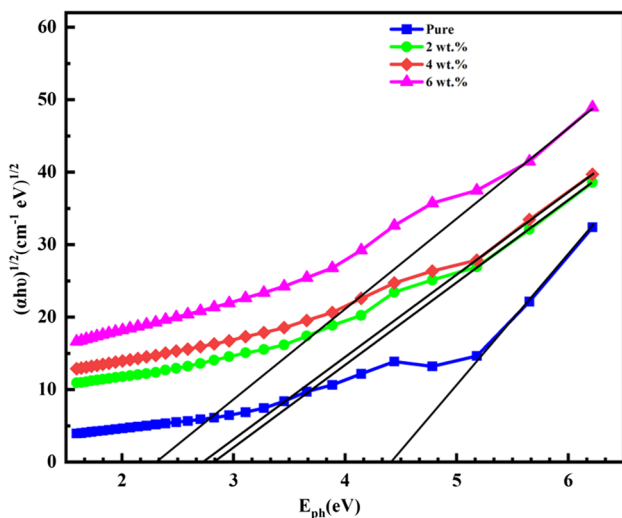
**Table 2** Values of energy gap for indirect transitions (forbidden and allowed) in the (PVA/SiO<sub>2</sub>-CuO) nanocomposites

Con. of (SiO <sub>2</sub> -CuO) nanoparticles wt.%	Indirect energy gap (allowed) eV	Indirect energy gap (forbidden) eV
0	4.40	3.73
2	2.81	1.35
4	2.72	1.26
6	2.31	1.05

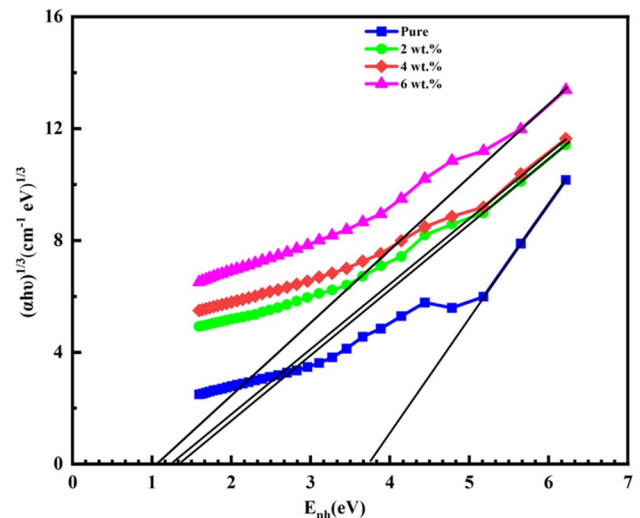
of disallowed indirect transitions are somewhat lower than those of allowed indirect transitions [48].

Figure 8 illustrates the relationship between the coefficient of extinction ( $k$ ) and the wavelength of the nanocomposite films composed of PVA/SiO<sub>2</sub>-CuO. The observed phenomenon of the extinction coefficient can be attributed to the significant absorbance exhibited by all nanocomposites. Furthermore, identical behavior was observed in visible and near-infrared spectral regions. The findings of this study indicate a notable enhancement in the performance of the nanocomposites due to the inclusion of SiO<sub>2</sub>-CuO nanoparticles. Notably, a higher ratio of SiO<sub>2</sub>-CuO in this investigation exhibited a consistent improvement in the outcomes compared to other nanocomposites. Additionally, an increase in the wavenumber, as depicted in Fig. 8, further supported these findings. At a wavelength of 780 nm, the findings demonstrated significant increases in the extinction coefficient by 668%, 970%, and 1680% as the concentrations of (SiO<sub>2</sub>-CuO) NPs in the nanocomposites increased by 2 wt.%, 4 wt.%, and 6 wt.%, respectively [49].

Figure 9 illustrates the relationships between the refractive index and the wavelength for polymer nanocomposite



**Fig. 6** Difference of  $(\alpha h\nu)^{1/2}$  for (PVA/SiO<sub>2</sub>-CuO) NCs with photon energy



**Fig. 7** Difference of  $(\alpha h\nu)^{1/3}$  of (PVA/SiO<sub>2</sub>-CuO) NCs with photon energy



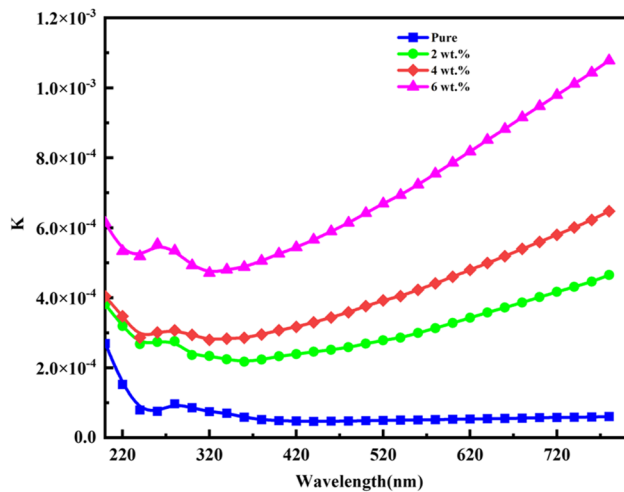


**Fig. 8** Difference of extinction coefficient for (PVA/SiO<sub>2</sub>-CuO) NCs with wavelength

films consisting of PVA/SiO<sub>2</sub>-CuO. The data demonstrate that the values of  $n$  exhibit an upward trend with the increasing concentration of SiO<sub>2</sub>-CuO nanoparticles. The high density observed in the nanocomposites can be attributed to the close packing of SiO<sub>2</sub>-CuO nanoparticles. The refractive index of pure polyvinyl alcohol (PVA) experiences an increase from 1.37 to 2.75 upon the introduction of 6 weight per cent of silicon dioxide-copper oxide (SiO<sub>2</sub>-CuO) nanoparticles into the PVA matrix. Figure 9 illustrates a notable decline in the refractive index as the wavelength in the visible region increases until it reaches a wavelength of 360 nm. Following this, the refractive index exhibits a very stable value within the 360 to 780 nm wavelength range. The link seen between the refractive index and the concentration of

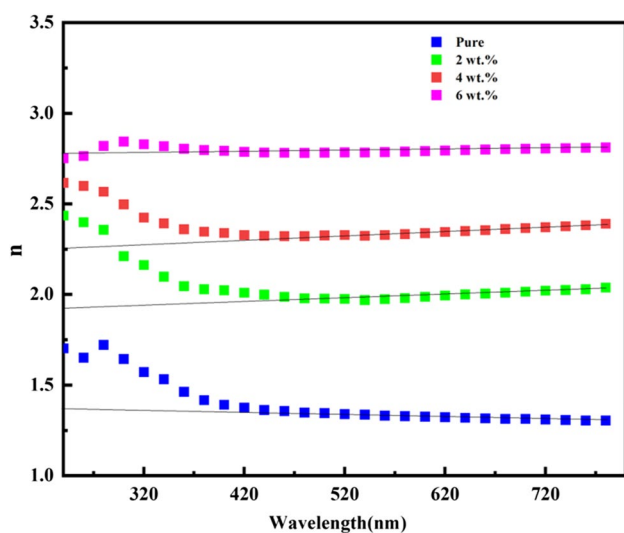


**Fig. 9** Refractive index for (PVA/SiO<sub>2</sub>-CuO) NCs as a function of wavelength

SiO<sub>2</sub>-CuO nanoparticles can be explained by the interaction between incident light and the polymer matrix that encompasses these nanoparticles. This interaction results in an elevated level of light refraction, augmenting the films' refractive properties [50].

Real dielectric constant  $\epsilon_1$  presented how much the speed of light was slowed down in the material, which is considered a measure of the polarity of a material. In contrast, imaginary dielectric constant  $\epsilon_2$  demonstrated the dielectric absorb energy by the electric field through the dipole motion [51]. Figures 10 and 11 illustrated the variation of real  $\epsilon_1$  and imaginary  $\epsilon_2$  parts of the dielectric constant for pure polymer and its nanocomposite films with different ratios of SiO<sub>2</sub>-CuO NPs as a function of wavelength. It can be observed that there is an increase in the values of  $\epsilon_1$  at low photonic energies followed by an apparent decrease in the higher energies for all nanocomposite films. The rise in the dielectric constant of polymers signifies a proportional augmentation in the charges present within the polymer materials [50]. The relationship between the real part of the dielectric constant and the refractive index is believed to be influenced by the small magnitude of the extinction coefficient. The empirical evidence indicates that there is a positive correlation between the concentrations of SiO<sub>2</sub>-CuO nanoparticles and the observed increase in the real dielectric constant. The observed behavior of the imaginary dielectric constant, both before and after the addition, exhibits similarities to that of the real dielectric constant. However, it is essential to note that the value of the imaginary dielectric constant is comparatively lower, as depicted in Fig. 11. The correlation between the imaginary component of the dielectric constant and the extinction coefficient is of significant

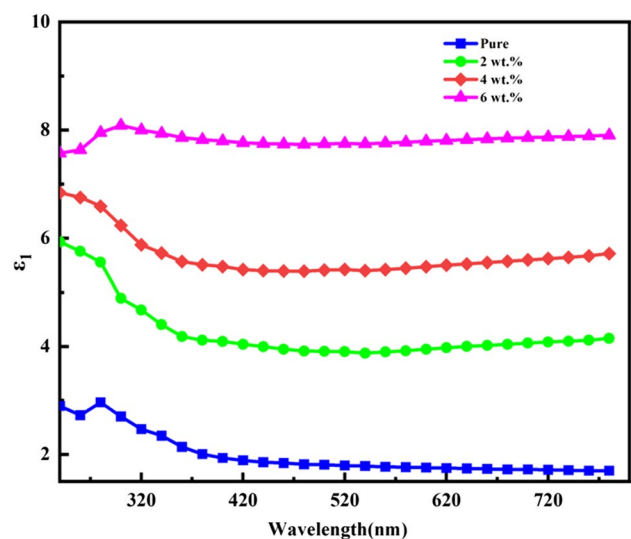


**Fig. 10** The real dielectric constant ( $\epsilon_1$ ) as a function of incident wavelength for (PVA/SiO<sub>2</sub>-CuO) NCs



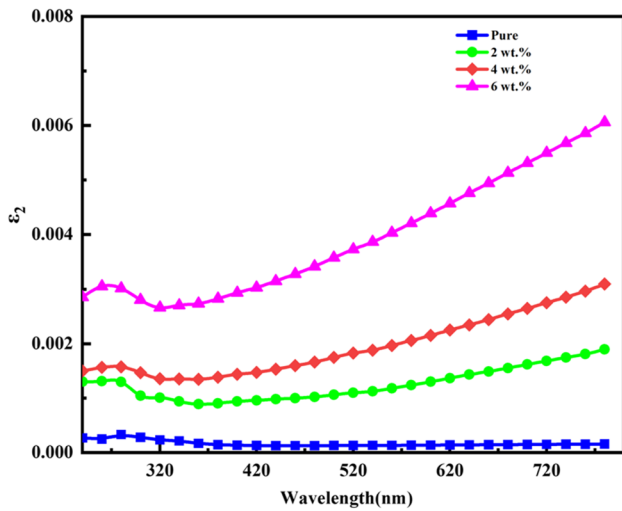


**Fig. 11** The imaginary dielectric constant ( $\epsilon_2$ ) as a function of wavelength for (PVA/SiO<sub>2</sub>-CuO) NCs

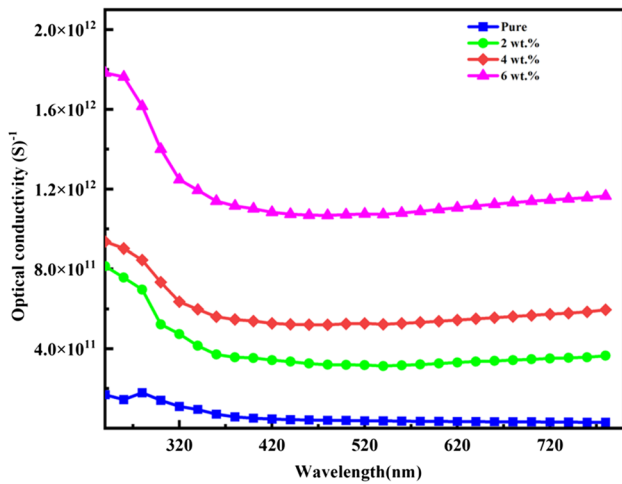


**Fig. 12** Difference of optical conductivity of (PVA/SiO<sub>2</sub>-CuO) NCs with wavelength

significance, particularly within the visible and near-infrared spectrums. In the context of this specific regime, it is evident that the refractive index exhibits a consistent and unchanging value, while the extinction coefficient exhibits an increasing trend with the increment in wavelength [52].

**Table 3** Shows comparison the experimental values of the optical properties of this work with other works

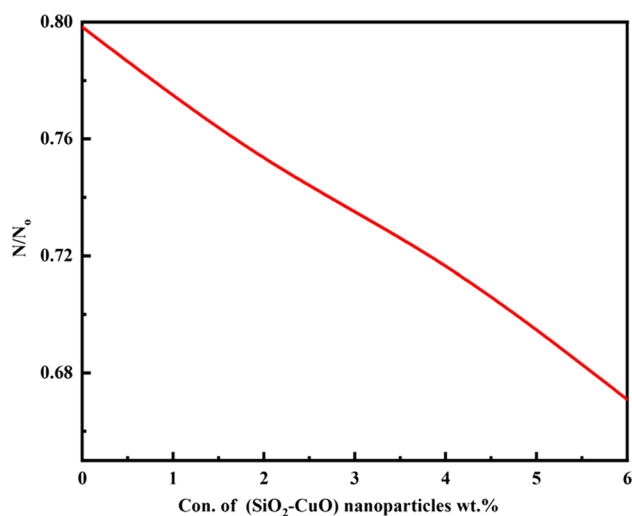
The optical properties	This work	Previous works
Indirect optical energy gap (allowed) eV	4.40 – 2.31 eV	3.9 – 2.3 eV [54]
Indirect optical energy gap (forbidden) eV	3.73 – 1.05 eV	3.8 – 1.13 eV [55]
Absorbance	0.05 – 2.7	1.1– 3 [56]
Refractive index	1.3 – 2.8	1.5 – 2.6 [55]
The real dielectric constant	1.8–8	1.5 – 7.6 [57]

Figure 12 illustrates the correlation between optical conductivity and wavelength in nanocomposites composed of polyvinyl alcohol (PVA) and silicon dioxide-copper oxide (SiO<sub>2</sub>-CuO). The optical conductivity of nanocomposites demonstrates a decline in magnitude with increasing wavelengths of light. The correlation between the optical conductivity and the wavelength of the incident radiation in the nanocomposite samples can explain the observed effect. The heightened optical conductivity found at shorter photon wavelengths can be attributed to the amplified absorbance of nanocomposites within that particular spectral region. An increase in the link between the concentration of nanoparticles and the optical conductivity of nanocomposites has been found. The behavior above can be attributed to localized energy levels within the energy gap, resulting in heightened absorption coefficients and optical conductivity [53]. Table 3 shows comparison the optical properties values with previous works.

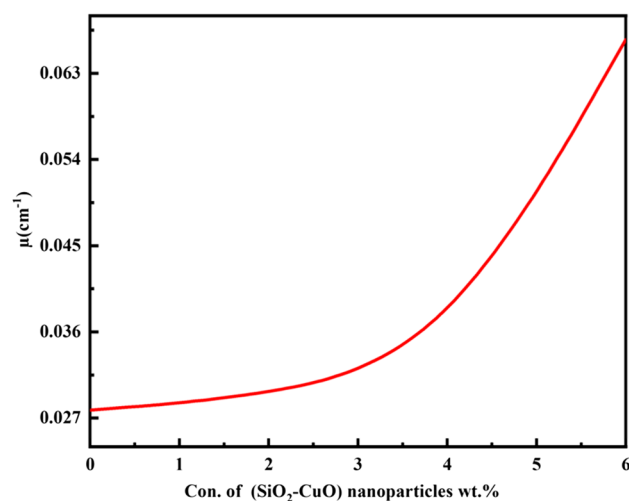
### 3.4 Application of (PVA/SiO<sub>2</sub>-CuO) NCs for Gamma Ray Shielding

Figure 13 illustrates the oscillations of ( $N/N_0$ ) in pure PVA with different concentrations of (SiO<sub>2</sub>-CuO) nanoparticles. The attenuation of radiation increases due to the rise in concentrations of (SiO<sub>2</sub>-CuO) nanoparticles, leading to a decrease in transmission radiation [58]. Figure 14 shows increasing  $\ln(N/N_0)$  of pure PVA with increases in (SiO<sub>2</sub>-CuO) NPs concentrations. The values obtained are presented in Table 4.

The graphical representation in Fig. 15 depicts the fluctuation in attenuation coefficients of gamma radiation concerning the concentrations of (SiO<sub>2</sub>-CuO) nanoparticles in a pure PVA. As documented in the reference, the escalation observed in attenuation coefficients with increasing nanoparticle concentrations can be attributed to the nanocomposite shielding materials' absorption or reflection of gamma radiation. Upon comparison, the outcomes of polymer nanocomposites and concrete, as depicted in the figure below, exhibited a high degree of similarity. The composite polymer exhibited superior properties to concrete owing to its enhanced mobility, absence of electrical conductivity, and potential to impede the escape of neutrons [59]. Table 4 shows values of  $N/N_0$ ,  $\ln N/N_0$  and  $\mu$  for (PVA/SiO<sub>2</sub>-CuO) NCs.



**Fig. 13** Variance of  $(N/N_0)$  for pure PVA with different concentrations of SiO<sub>2</sub>-CuO NPs



**Fig. 15** Variance of attenuation coefficients of gamma radiation for pure PVA with different concentrations of SiO<sub>2</sub>-CuO nanoparticles

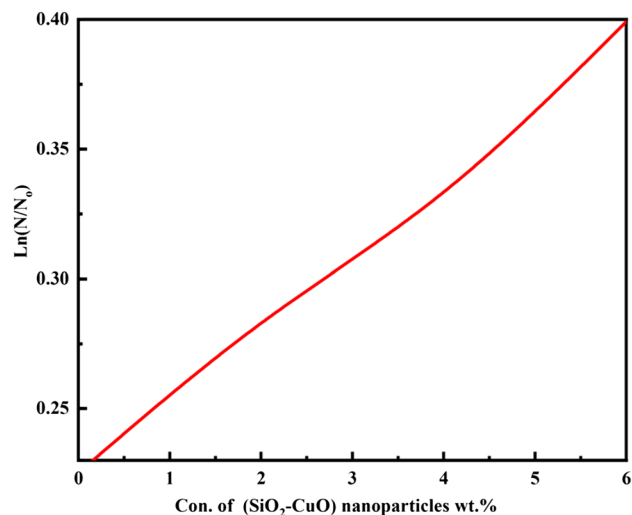


**Fig. 14** Change of  $\ln(N/N_0)$  for pure PVA with different concentrations of SiO<sub>2</sub>-CuO nanoparticles

**Table 4** Values of  $N/N_0$ ,  $\ln N/N_0$ , and  $\mu$  for (PVA/SiO<sub>2</sub>-CuO) NCs

Con. of (SiO <sub>2</sub> -CuO) nanoparticles wt.%	$N/N_0$	$\ln N/N_0$	$\mu(\text{cm}^{-1})$
0	0.79	0.22	0.027
2	0.75	0.28	0.029
4	0.71	0.33	0.033
6	0.67	0.39	0.066

## 4 Conclusion

The current study involves the production of nanostructured films composed of polyvinyl alcohol (PVA) and a combination of silicon dioxide (SiO<sub>2</sub>) and copper oxide (CuO) by the solution casting method. The investigation focused on analyzing the structural and optical characteristics of nanostructures composed of polyvinyl alcohol (PVA) and silicon dioxide-copper oxide (SiO<sub>2</sub>-CuO). The utilization of nanostructures composed of polyvinyl alcohol (PVA) and silicon dioxide (SiO<sub>2</sub>) with copper oxide (CuO) is prevalent in the field of optical nanodevices and gamma ray shielding. FTIR spectra indicate the presence of a physical interaction between the pristine polymer and (SiO<sub>2</sub>-CuO) nanoparticles. The optical microscope photos indicate that the dispersion of (SiO<sub>2</sub>-CuO) additions exhibited homogeneity, and the nanoparticles formed a coherent network within the polymer blend. The augmentation in the concentration of nanoparticles comprising silicon dioxide and copper oxide (SiO<sub>2</sub>-CuO) results in an elevation of both the absorbance and absorption coefficient of nanocomposites composed of polyvinyl alcohol and SiO<sub>2</sub>-CuO (PVA/SiO<sub>2</sub>-CuO). The observed rise in the refractive index, extinction coefficient, dielectric constant (both real and imaginary), and optical conductivity is directly proportional to the concentration of (SiO<sub>2</sub>-CuO). Incorporating a 6 wt.% concentration of (SiO<sub>2</sub>-CuO), the nanofiller reduced the energy gap associated with both indirect transitions, whether allowed or forbidden. In particular, there was a drop in the energy gap for permissible transitions from 4.40 to 2.31 electron volts (eV), and the energy gap for impermissible transitions reduced from 3.73 to 1.05 eV.

Moreover, a higher SiO<sub>2</sub>-CuO ratio leads to a reduction in transmittance. Finally, the attenuation coefficient rises for gamma radiation with increased concentration of (SiO<sub>2</sub>-CuO) nanoparticles. The study's findings indicate that the (PVA/SiO<sub>2</sub>-CuO) nanocomposite, when used as a lead-free material, has favorable shielding properties against gamma rays; this suggests that it has the potential to serve as a viable alternative to conventional radiation shielding materials in the field of nuclear medicine. The sample with a concentration of 6% exhibited a higher level of performance in comparison to the remaining samples; this is supported by the observed attenuation coefficient, which exhibited a 133% increase compared to the attenuation coefficient of the pure sample. Furthermore, the sample possesses an impressive bandgap, rendering it appropriate for use in various electronic devices.

**Acknowledgements** Acknowledgements to University of Babylon

**Author Contributions** All authors contributed to the study's conception and design. Material preparation, data collection and analysis were performed by Idrees Oreibi, Majeed Ali Habeeb and Rehab Shather Abdul Hamza. The first draft of the manuscript was written by Majeed Ali Habeeb and all authors commented on previous versions of the manuscript. All authors read and approved the final manuscript.

**Funding** None.

**Data Availability** Available.

## Declarations

**Competing interests** The authors declare no competing interests.

**Ethics Approval** The research is not involving the studies on human or their data.

**Consent to Participate** Consent.

**Consent for Publication** Consent.

## References

1. Bezza FA, Tichapondwa SM, Chirwa EM (2020) Fabrication of monodispersed copper oxide nanoparticles with potential application as antimicrobial agents. *Sci Rep* 10(1):16680
2. Hadi AH, Habeeb MA (2021) The dielectric properties of (PVA-PVP-CdS) nanocomposites for gamma shielding applications. *J Phys Conf Ser* 1973(1):012063. <https://doi.org/10.1088/1742-6596/1973/1/012063>
3. Hashim A, Habeeb MA, Jebur QM (2020) Structural, dielectric and optical properties for (Polyvinyl alcohol-polyethylene oxide manganese oxide) nanocomposites. *Egypt J Chem* 63:735–749. <https://doi.org/10.21608/ejchem.2019.14849.1901>
4. Cha J, Kim J, Ryu S, Hong SH (2019) Comparison to mechanical properties of epoxy nanocomposites reinforced by functionalized carbon nanotubes and graphene nanoplatelets. *Compos B Eng* 162:283–288
5. Choudhary S (2018) Characterization of amorphous silica nano-filler effect on the structural, morphological, optical, thermal, dielectric and electrical properties of PVA–PVP blend based polymer nanocomposites for their flexible nanodielectric applications. *J Mater Sci Mater Electron* 29:10517–10534
6. Abdul Hamza RS, Habeeb MA (2023) Synthesis and tuning the structural, morphological and dielectric characteristics of PVA-CMC-SiO<sub>2</sub>-Cr<sub>2</sub>O<sub>3</sub> hybrid nanostructures for nanoelectronics devices. *Opt Quant Electron* 55(8):705. <https://doi.org/10.1007/s11082-023-04995-3>
7. Jebur QM, Hashim A, Habeeb MA (2020) Structural, A.C electrical and optical properties of (polyvinyl alcohol-polyethylene oxide-aluminum oxide) nanocomposites for piezoelectric devices. *Egypt J Chem* 63:719–734. <https://doi.org/10.21608/ejchem.2019.14847.1900>
8. Mohamed MB, Abdel-Kader MH (2019) Effect of excess oxygen content within different nano-oxide additives on the structural and optical properties of PVA/PEG blend. *Appl Phys A* 125(3):1–11
9. Habeeb MA, Hashim A, Hayder N (2020) Fabrication of (PS-Cr<sub>2</sub>O<sub>3</sub>/ZnCoFe<sub>2</sub>O<sub>4</sub>) nanocomposites and studying their dielectric and fluorescence properties for IR sensors. *Egypt J Chem* 63:709–717. <https://doi.org/10.21608/ejchem.2019.13333.1832>
10. Ping Z, Nguyen QT, Essamri A, Ne el J (1994) *Polym Adv Technol Macromol Chem Phys* (195):21-31
11. Sreekanth K, Siddaiah T, Gopal NO, Madhava Kumar Y, Ramu CH (2019) Optical and electrical conductivity studies of VO<sub>2</sub>+doped Polyvinyl pyrrolidone (PVP) polymer electrolytes. *J Sci Adv Mater Devices* ISBN 4:230–236
12. Habeeb MA, Mahdi WS (2019) Characterization of (CMC-PVP-Fe<sub>2</sub>O<sub>3</sub>) nanocomposites for gamma shielding application. *Int J Emerg Trends Eng Res* 7(9):247–255. <https://doi.org/10.30534/ijeter/2019/06792019>
13. Gaabour LH (2019) Influence of silica nanoparticles incorporated with chitosan/polyacrylamide polymer nanocomposites. *J Market Res* 8(2):2157–2163
14. Mahdi SM, Habeeb MA (2022) Fabrication and tailored structural and dielectric characteristics of (SrTiO<sub>3</sub>/ NiO ) nanostructure doped (PEO/PVA) polymeric blend for electronics fields. *Phys Chem Solid State* 23(4):785–792. <https://doi.org/10.15330/pcss.23.4.785-792>
15. Al-Sharifi NK, Habeeb MA (2023) Improvement structural and dielectric properties of PS/SiC/Sb<sub>2</sub>O<sub>3</sub> nanostructures for nanoelectronicss devices. *East Eur J Phys* 2:341–347. <https://doi.org/10.26565/2312-4334-2023-2-40>
16. Mohammed AA, Habeeb MA (2023) Effect of Si<sub>3</sub>N<sub>4</sub>/TaC nanomaterials on the structural and electrical characteristics of poly methyl methacrylate for electrical and electronics applications. *East Eur J Phys* 2:157–164. <https://doi.org/10.26565/2312-4334-2023-2-15>
17. Soliman T, Vshivkov S (2019) Effect of Fe nanoparticles on the structure and optical properties of polyvinyl alcohol nanocomposite films. *J Non-Cryst Solids* 519:119452
18. Micozzi MS, Townsend FM, Koop CE (1990) From Army Medical Museum to national museum of health and medicine. A century-old institution on the move. *Arch Pathol Lab Med* 114(12):1290–1295
19. Chopra KL, Paulson PD, Dutta V (2004) Thin film solar cells: an overview. *Prog Photovoltaics Res Appl* 12(2):69–92
20. Tauc J, Menth A, Wood DL (1970) Optical and magnetic investigations of the localized states in semiconducting glasses. *Phys Rev Lett* 25(11):749–961
21. Alshehri A, Salim E, Oraby A (2021) Structural, optical, morphological and mechanical studies of polyethylene oxide/sodium alginate blend containing multi-walled carbon nanotubes. *J Market Res* 15:5615–5622

22. Habeeb MA, Hamza RSA (2018) Synthesis of (polymer blend –MgO) nanocomposites and studying electrical properties for piezoelectric application. *Indones J Electr Eng Inform* 6(4):428–435. <https://doi.org/10.11591/ijeel.v6i1.511>
23. Abulyazied D, Saudi H, Zakaly HM, Issa SA, Henaish A (2022) Novel nanocomposites based on polyvinyl alcohol and molybdenum nanoparticles for Gamma irradiation shielding. *Opt Laser Technol* 156:108560
24. Jaber ZS, Habeeb MA, Radi WH (2023) Synthesis and Characterization of (PVA-CoO-ZrO<sub>2</sub>) Nanostructures for Nanooptoelectronic Fields. *East Eur J Phys* 2:228–233
25. Alhazime AA (2020) Effect of nano CuO doping on structural, thermal and optical properties of PVA/PEG blend. *J Inorg Organomet Polym Mater* 30:4459–4467
26. Mahdi SM, Habeeb MA (2022) Synthesis and augmented optical characteristics of PEO-PVA-SrTiO<sub>3</sub>-NiO hybrid nanocomposites for optoelectronics and antibacterial applications. *Opt Quant Electron* 54(12):854. <https://doi.org/10.1007/s11082-022-04267-6>
27. Habeeb MA (2014) Dielectric and optical properties of (PVAc-PEG-Ber) biocomposites. *J Eng Appl Sci* 9(4):102–108. <https://doi.org/10.36478/jeasci.2014.102.108>
28. Aldeen LT, Naser BK, Ali A, Abdulridha AR, Abbas TM, Naser BA (2022) Effect of laser organic dyes on the optical properties of (PVA-PEG) blend. *Neuro Quantology J* 20(8):5524–5530
29. Habeeb MA (2011) Effect of rate of deposition on the optical parameters of GaAs films. *Eur J Sci Res* 57(3):478–484
30. Habeeb MA, Hashim A, Hayder N (2020) Structural and optical properties of novel (PS-Cr<sub>2</sub>O<sub>3</sub>/ZnCoFe<sub>2</sub>O<sub>4</sub>) nanocomposites for UV and microwave shielding. *Egypt J Chem* 63:697–708. <https://doi.org/10.21608/ejchem.2019.12439.1774>
31. Du H, Xu GQ, Chin WS, Huang L, Ji W (2002) Synthesis, characterization, and nonlinear optical properties of hybridized CdS-polystyrene nanocomposites. *Chem Mater* 14(10):4473–4479. <https://doi.org/10.1021/cm010622z>
32. Habeeb MA, Hashim A, Hayder N (2020) Structural and optical properties of novel (PS-Cr<sub>2</sub>O<sub>3</sub>/ZnCoFe<sub>2</sub>O<sub>4</sub>) nanocomposites for UV and microwave shielding. *Egypt J Chem* 63:697–708. <https://doi.org/10.21608/ejchem.2019.12439.1774>
33. Mahdi SM, Habeeb MA (2023) Low-cost piezoelectric sensors and gamma ray attenuation fabricated from novel polymeric nanocomposites. *AIMS Mater Sci* 10(2):288–300. <https://doi.org/10.3934/matasci.2023015>
34. Habeeb MA, Kadhim WK (2014) Study the optical properties of (PVA-PVAc-Ti) nanocomposites. *J Eng Appl Sci* 9(4):109–113. <https://doi.org/10.36478/jeasci.2014.109.113>
35. Liu P, Chen W, Liu C, Tian M, Liu P (2019) A novel poly (vinyl alcohol)/poly (ethylene glycol) scaffold for tissue engineering with a unique bimodal open-celled structure fabricated using supercritical fluid foaming. *Sci Rep* 9(1):9534
36. Luo Q, Shan Y, Zuo X, Liu J (2018) Anisotropic tough poly (vinyl alcohol)/graphene oxide nanocomposite hydrogels for potential biomedical applications. *RSC Adv* 8(24):13284–13291
37. Habeeb MA, Al-Sharifi NK, Mohammed AA (2023) Fabrication and exploring the structural, dielectric and optical features of PVA/SnO<sub>2</sub>/Cr<sub>2</sub>O<sub>3</sub> nanostructures for optoelectronic applications. *Opt Quant Electron* 55(11):1016. <https://doi.org/10.1007/s11082-023-05261-2>
38. Habeeb MA, Jaber ZS (2022) Enhancement of structural and optical properties of CMC/PAA blend by addition of zirconium carbide nanoparticles for optics and photonics applications. *East Eur J Phys* 4:176–182. <https://doi.org/10.26565/2312-4334-2022-4-18>
39. Mahdi SM, Habeeb MA (2023) Tailoring the structural and optical features of (PEO-PVA)/(SrTiO<sub>3</sub>-CoO) polymeric nanocomposites for optical and biological applications. *Polym Bull.* <https://doi.org/10.1007/s00289-023-04676-x>
40. Shubha A, Manohara SR, Gerward L (2017) Influence of polyvinylpyrrolidone on optical, electrical, and dielectric properties of poly (2-ethyl-2-oxazoline)-polyvinylpyrrolidone blends. *J Mol Liq* 247:328–336
41. Dwech MH, Habeeb MA, Mohammed AH (2022) Fabrication and evaluation of optical characteristic of (PVA-MnO<sub>2</sub>-ZrO<sub>2</sub>) nanocomposites for nanodevices in optics and photonics. *Ukr J Phys* 67(10):757–762. <https://doi.org/10.15407/ujpe67.10.757>
42. Mohammed AA, Habeeb MA (2023) Modification and development of the structural, optical and antibacterial characteristics of PMMA/Si<sub>3</sub>N<sub>4</sub>/TaC nanostructures. *Silicon.* <https://doi.org/10.1007/s12633-023-02426-2>
43. Al-Sharifi NK, Habeeb MA (2023) Synthesis and exploring structural and optical properties of ternary PS/SiC/Sb<sub>2</sub>O<sub>3</sub> nanocomposites for optoelectronic and antimicrobial applications. *Silicon.* <https://doi.org/10.1007/s12633-023-02418-2>
44. Yu SH, Yoshimura M, Moreno JMC, Fujiwara T, Fujino T, Teranishi R (2001) In situ fabrication and optical properties of a novel polystyrene/semiconductor nanocomposite embedded with CdS nanowires by a soft solution processing route. *Langmuir* 17(5):1700–1707. <https://doi.org/10.1021/la000941p>
45. Hayder N, Habeeb MA, Hashim A (2020) Structural, optical and dielectric properties of (PS-In<sub>2</sub>O<sub>3</sub>/ZnCoFe<sub>2</sub>O<sub>4</sub>) nanocomposites. *Egypt J Chem* 63:577–592. <https://doi.org/10.21608/ejchem.2019.14646.1887>
46. Rajesh K, Crasta V, Rithin Kumar N, Shetty G, Rekha P (2019) Structural, optical, mechanical and dielectric properties of titanium dioxide doped PVA/PVP nanocomposite. *J Polym Res* 26(4):1–10
47. Hadi AH, Habeeb MA (2021) Effect of CdS nanoparticles on the optical properties of (PVA-PVP) blends. *J Mech Eng Res Dev* 44(3):265–274. <https://jmerd.net/03-2021-265-274/>
48. Habeeb MA, Abdul Hamza RS (2018) Novel of (biopolymer blend-MgO) nanocomposites: Fabrication and characterization for humidity sensors. *J Bionanoscience* 12(3):328–335. <https://doi.org/10.1166/jbns.2018.1535>
49. Manhas SS, Rehan P, Kaur A, Acharya AD, Sarwan B (2019) Evaluation of optical properties of polypyrrole: Polystyrene nanocomposites. *AIP Conf Proc* 2100(April):1–5. <https://doi.org/10.1063/1.5098591>
50. Sabur DA, Habeeb MA, Hashim A (2023) Fabrication and tailoring the structural and dielectric characteristics of G.O./Sb<sub>2</sub>O<sub>3</sub>/PMMA/PC quaternary nanostructures for solid state electronics nanodevices. *Phys Chem Solid State* 24(1):173–180
51. Mahdi SM, Habeeb MA (2022) Evaluation of the influence of SrTiO<sub>3</sub> and CoO nanofillers on the structural and electrical polymer blend characteristics for electronic devices. *Dig J Nanomater Biostructures* 17(3):941–948. <https://doi.org/10.15251/DJNB.2022.173.941>
52. Habeeb MA, Mohammed AH (2023) Fabrication and tailored optical and electrical characteristics of Co<sub>2</sub>O<sub>3</sub>/SiC nanostructures doped PVA for multifunctional technological applications. *Opt Quant Electron* 55(9):791. <https://doi.org/10.1007/s11082-023-05061-8>
53. Vidyalaya KM (2009) Analysis of electrical properties of Li<sup>3+</sup> ion beam irradiated lexan polycarbonate also act as catalyst to speed up the discoloration. The formation of conjugated. *Asian J Chem* 21(10):43–46
54. Sabur DA, Hashim A, Habeeb MA (2023) Fabrication and exploration the structural and optical properties of Sb<sub>2</sub>O<sub>3</sub>-GO nanostructures doped PMMA-PC for photodegradation of pollutants dyes 55(5): 457. <https://doi.org/10.1007/s11082-023-04726-8>
55. Hashim A, Alshrefi SM, Abed HH, Hadi A (2023) Synthesis and boosting the structural and optical characteristics of PMMA/SiC/CdS hybrid nanomaterials for future optical and nanoelectronics



- applications. *J Inorg Organomet Polym Mater* 1–9. <https://doi.org/10.1007/s10904-023-02866-8>
56. Hamza RSA, Habib MA (2023) Reinforcement of morphological, structural, optical, and antibacterial characteristics of PVA/CMC bioblend filled with SiO<sub>2</sub>/Cr<sub>2</sub>O<sub>3</sub> hybrid nanoparticles for optical nanodevices and food packing industries. *Polymer Bulletin* 1–22. <https://doi.org/10.1007/s00289-023-04913-3>
57. Hashim A, Hadi A, Al-Aaraji NA-H (2023) Fabrication and augmented electrical and optical characteristics of PMMA/CoFe<sub>2</sub>O<sub>4</sub>/ZnCoFe<sub>2</sub>O<sub>4</sub> hybrid nanocomposites for quantum optoelectronics nanosystems. *Opt Quant Electron* 55(8):716
58. Habib MA, Rahdi WH (2023) Titanium carbide nanoparticles filled PVA-PAAm nanocomposites, structural and electrical characteristics for application in energy storage. *Opt Quant Electron* 55(4):334. <https://doi.org/10.1007/s11082-023-04639-6>
59. Liang GD, Tjong SC (2008) Electrical properties of percolative polystyrene/carbon nanofiber composites. *IEEE Trans Dielectr Electr Insul* 15(1):214–220. <https://doi.org/10.1109/T-DEI.2008.4446753>

**Publisher's Note** Springer Nature remains neutral with regard to jurisdictional claims in published maps and institutional affiliations.

Springer Nature or its licensor (e.g. a society or other partner) holds exclusive rights to this article under a publishing agreement with the author(s) or other rightsholder(s); author self-archiving of the accepted manuscript version of this article is solely governed by the terms of such publishing agreement and applicable law.